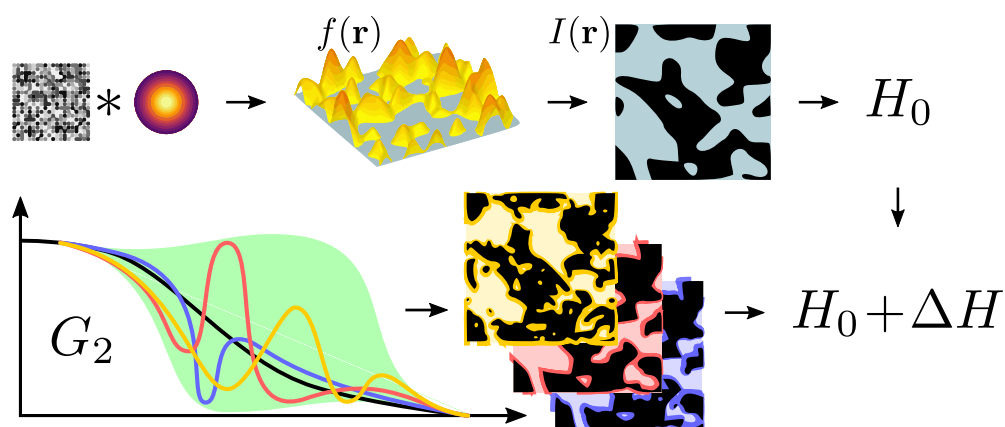


Graphical Abstract

Towards effective information content assessment: analytical derivation of information loss in the reconstruction of random fields with model uncertainty

Aleksei Cherkasov, Kirill M. Gerke, Aleksey Khlyupin



Highlights

Towards effective information content assessment: analytical derivation of information loss in the reconstruction of random fields with model uncertainty

Aleksei Cherkasov, Kirill M. Gerke, Aleksey Khlyupin

- Shannon entropy for random fields with model uncertainty can be explicitly expressed by developed theoretical model
- Stochastic perturbation of fields' correlation function decreases its information content
- Different regions of correlation function are in different extent informative and sensitive for perturbation
- Proposed model bridges the gap between descriptor-based heterogeneous media reconstruction and information theory

Towards effective information content assessment: analytical derivation of information loss in the reconstruction of random fields with model uncertainty

Aleksei Cherkasov^a, Kirill M. Gerke^{b,*}, Aleksey Khlyupin^{a,b}

*^aMoscow Institute of Physics and Technology, Institutskiy Pereulok
9, Dolgoprudny, 141700, Russia*

*^bSchmidt Institute of Physics of the Earth of Russian Academy of Sciences, Bolshaya
Gruzinskaya 10, Moscow, 123242, Russia*

Abstract

Structures are abundant in both natural and human-made environments and usually studied in the form of images or scattering patterns. To characterize structures a huge variety of descriptors is available spanning from porosity to radial and correlation functions. In addition to morphological structural analysis, such descriptors are necessary for stochastic reconstructions, stationarity and representativity analysis. The most important characteristic of any such descriptor is its information content - or its ability to describe the structure at hand. For example, from crystallography it is well known that experimentally measurable S_2 correlation function lacks necessary information content to describe majority of structures. The information content of this function can be assessed using Monte-Carlo methods only for very small 2D images due to computational expenses. Some indirect quantitative approaches for this and other correlation function were also proposed. Yet, to date no methodology to obtain information content for arbitrary 2/3D image is available. In this work, we make a step toward developing a general framework to perform such computations analytically. We show, that one can assess the entropy of a perturbed random field and that stochastic perturbation of fields' correlation function decreases its information content. In addition to analytical expression, we demonstrate that different regions of correlation function are in different extent informative

*Corresponding author

Email address: kg@ifz.ru (Kirill M. Gerke)

and sensitive for perturbation. Proposed model bridges the gap between descriptor-based heterogeneous media reconstruction and information theory and opens way for computationally effective way to compute information content of any descriptor as applied to arbitrary structure.

Keywords: correlation functions, structure characterization, structural descriptors, image analysis, information content

1. Introduction

Structures, or spatial arrangements of some matter or phases, are ubiquitous in nature, and, thus, a target of studies in numerous research areas. Examples may include galaxy formations [1], immiscible multi-phase fluid flow patterns [2, 3], rock and soil samples [4, 5, 6, 7, 8], food specimens [9, 10] or biological tissue [11]. The scale of interest may span orders of magnitude from as small as couple of nm for nanoporous materials [12, 13] to millions of light-years for star clusters [14]. Studied structures are not necessarily static and may exhibit temporal variation in their arrangement [15, 16] which can be a result of interacting with surrounding material. Closed or open, one needs to characterize such systems of structures in order to assess their physical properties [17, 18] - an ultimate goal needed to describe complex behavior of studied systems with numerical models. A wide varieties of descriptors were developed in order to quantify spatial structure, for example: phase ratio or porosity, surface area, radial distribution functions [19, 20], Minkowski functionals [21] and tensors [22], correlation functions [23] among numerous others]. Holy wars on the question which metric is superior still abound e.g.,[24, 25]. In reality, this issue boils down to a single characteristic.

The universal characteristic of any descriptor for structures is information content - the measure of the extend the given metric describes given structure. The challenge that explains the above-mentioned diversity of structural metrics is, however, the complexity in its evaluation. But let us start from the simplest example of porosity for a binary structure containing only pores and solid material. The information content in this case can be computed as:

$$I_{porosity} = N - \log_2(N_{pores}^N). \quad (1)$$

This represents a very simple idea that if we have a binary image and know its size then $I = -\log_2(p) = N$ (any realization of the structure is evenly distributed with the probability of $p = 1/N^2$), where N is the total number of pixels (i.e., the size of the image) and logarithm insures that information content is expressed in bits (i.e., one bit per pixel). Now if in addition to that we know the porosity (phase ratio of pore to solid pixels on the image), we simply obtain Eq.1 by substituting the amount of information contained in specifying the value of N_{pores} [26], as opposed to knowing only the system size. Here we immediately come to a number of important observations: 1) the information content of porosity alone is rather small (which explains the doomed to fail quest to predict physical properties such as permeability from porosity values [27, 28] and very poor performance of Kozeny-Carman like relationships [29, 30]) for anything different from sphere packings in general, and 2) it varies with the value of porosity with the maximum at 0.5 (like porosity any metric may change its content with small alterations in the structure itself). But before we move on to some more involved examples, the notion of stochastic reconstructions is in order.

The classical example of information content in action is the so-called crystallography problem. The standard correlation function S_2 can be measured from small angle scattering experiments [31] and it can be used to stochastically reconstruct the studied structure. A variety of techniques can be applied to recover the structure based on its autocorrelation [32] among which truncated random Gaussian fields was one of the pioneering approaches [33]. It was immediately recognized that S_2 alone is not enough to recover the measured structure. Gaussian random field, for example, can produce numerous realizations of the same auto-correlation function that are all valid solutions. Such solutions are called degenerate states. As later became clear with the progress in stochastic reconstruction methods, the problem is even deeper- not only we are not aware which realization is the target one, but stochastic reconstructions preferentially converge to a limited amount of solutions [34, 35]. Interestingly, the latter is also true to reconstruction techniques not based on correlation functions which include multiple-point statistics [36, 37, 38] and deep learning methods [39, 40]. To summarize, autocorrelation, while much more informative than porosity, is not enough to describe any but the simplest of structures [26]; one needs to increase the information content of metrics used for stochastic reconstructions in order to improve their accuracy.

Increasing the information content of structural metrics is convoluted, as

it involves a trade-off between the amount of information and complexity of computation combined with the size of the metric. It is well recognized that n -point correlation function completely describes any structure. However, it has basically the size of structural image itself. For example, full correlation map of 2-point statistics is known to be enough to perform the stochastic reconstruction exactly [41, 42], but its size is four-times the original for 2D image. As adepts of correlation functions, we shall use them in this work; moreover, we argue that compared to other metrics they possess a number of important qualities: 1) in addition to sampling from images some correlation functions can be measured from experiments [31, 43, 44]; 2) a set of classical correlation functions [23] contains all conventional metrics [45], 3) unlike mainly scalar metrics, correlation functions can be computed in directions [46, 47] and, thus, account for structural anisotropy, 4) the order of correlation functions is useful measure of their information potential with full correlation map serving as 100% reference. This does not mean that information content can not be established for other metrics - it does and Eq.1 provides an example. Multiple-point statistics produces results resembling the original structure better if the size of the training window is enlarged (i.e., n -pointness is increased). It was also demonstrated that increasing the order of functions from 2-point to n -point have diminishing returns with each step [48, 26]. The trick is to utilize light-weight metrics that describe different aspects of structure. In practice this means using different correlation functions with low order, for example, S_2 , L_2 and two-point surface functions [49, 50, 51]. It was shown that the usage of cluster C_2 functions adds a lot of information, but its usage in reconstructions [52] is cumbersome due to computationally ineffective optimization in its recalculations for annealing updates. While considerable speed gains were achieved with hierarchical annealing [53, 54], what is the best order and number of correlation functions that should be used to reconstruct the structure at hand is still an open question. All this highlights the importance of solving the information content problem.

The straightforward way to assess information content is enumerate all possible structures that all satisfy the same correlation function or a set of correlation functions. This can be achieved by exploring the energy landscape of the stochastic reconstruction problem [55] and was applied to S_2 correlation function [56] in a similar manner we analyzed all possible variations for a given porosity value and image size in Eq.1. As we shall analyze later on, this is a very computationally expensive procedure that prohibits its

usage for arbitrary structure and set of functions. Other indirect approaches allow only qualitative estimates based on reconstructions [57] or analysis of specific Debye-type of structures [58]. In other words, we are still missing a universal and computationally effective approach to quantify information content. Information content evaluation is needed not only for stochastic reconstructions. Physical properties of any material depend on its structure, the boundary conditions [17, 59, 60, 61] and representativeness. The latter quality is tricky, but in many cases crucial to evaluate [62, 63, 64]. Strictly speaking, only statistically homogeneous structures can be representative. Choosing descriptors with sufficient information content for (in)homogeneity characterization is also important for stochastic reconstructions [65, 66, 67], structure compression [68, 69] and extracting features for machine learning [70, 71, 72]. In order to establish spatial stationarity one needs high information content [73], as otherwise the degenerate states may render homogeneity to be established incorrectly (false positive cases of stationarity [63]).

In light of the overall introductory discussion it seems that different structural descriptors have appeared in wide variety of research disciplines due to historical and ease of measuring reasons. To tame this motley of concepts and visions requires solving the problem of efficient information content evaluation for arbitrary structures. In this light, the aim of this paper is to develop an analytical approach to compute entropy for digital image after some perturbation to its descriptors is introduced. We believe this achievement to be a crucial step towards computing information content for any arbitrary structural descriptor at hand.

2. Theoretical Model

We consider random fields \mathbf{f} that can be sampled knowing the underlying probability model $P(\mathbf{f})$. Since the possible value of the field at each space point runs through a series of continuous values, then, strictly speaking, the number of different realizations of random fields \mathbf{f} is infinite. Therefore, the Shannon entropy [74] of such random fields is of interest as a measure of the information contained in their probabilistic model $P(\mathbf{f})$.

More specifically, our goal is the investigation of the uncertainty introduced into the underlying probabilistic model. If we add a random perturbation U to any parameter θ that determine the probability $P(\mathbf{f}; \theta + U)$, then the entropy growth of original fields \mathbf{f} is expected. This is pretty clear, since we have lost some information while adding such uncertainty which obeys

its own probability law $\rho(U)$. Thus, in this paper, we are interested in a quantitative estimate of such an additional Shannon entropy introduced into the system due to uncertainty.

In our model Gaussian fields \mathbf{f} are considered with a given arbitrary correlation matrix \hat{G}_2 . A random symmetric matrix \hat{U} added to the original matrix \hat{G}_2 acts as a small perturbation in the model. We show that one of the simple ways to investigate the additional entropy is to apply an orthogonal decomposition of random fields known as the Karhunen–Loève transform [75]. By combining this approach with matrix perturbation theory the desired expression for the entropy can be obtained, which is demonstrated below during step by step calculations. Our theoretical evaluation consists of three main steps. Firstly, we evaluate joint probability in the case of small perturbation of certain correlation matrix in the basis of correlation matrix eigenvectors. After that we provide the perturbation approach for Shannon information entropy using previous evaluations. Finally, desired expression for additional entropy is obtained making use of some averaging over random matrix probability model.

2.1. The Karhunen–Loève Transform for Random Fields

Arbitrary random field can be decomposed into a series in terms of an orthogonal functional basis using the Karhunen–Loève transform. For any finite number of terms this decomposition is the best in the sense of Euclidean norm of difference between the field and its approximation [75]. KLT and its discrete version (also commonly known as principal component analysis - PCA) have a wide range of applications such as bioinformatics [76], [77], data analysis [78], dimensionality reduction methods for direct [79], [80] and inverse problems [81], [82] of high computational complexity, applications in quantum physics and quantum information theory [83].

It will be convenient to provide our further perturbation analysis based on the KLT of random fields. So here we briefly introduce the KLT in the case of the non-perturbed correlation function G_2 which characterises a certain ensemble of Gaussian random fields $\mathbf{f}(\mathbf{r})$. The correlation function G_2 given by

$$G_2(\mathbf{x}) = G_2(|\mathbf{x}|) = \langle f(\mathbf{r})f(\mathbf{r} + \mathbf{x}) \rangle \quad (2)$$

corresponds to the unperturbed correlation matrix

$$(\hat{G}_2)_{ij} = G_2(\mathbf{r}_i - \mathbf{r}_j) = G_2(|\mathbf{r}_i - \mathbf{r}_j|) \quad (3)$$

The set of correlated variables $\mathbf{f} = [f(\mathbf{r}_1), \dots, f(\mathbf{r}_n)]^T$ has the joint probability density

$$\rho(\mathbf{f}) = \frac{|\hat{G}_2|^{-\frac{1}{2}}}{(2\pi)^{\frac{n}{2}}} \exp\left(-\frac{1}{2}\mathbf{f}^T \hat{G}_2^{-1} \mathbf{f}\right) \quad (4)$$

Due to the Karhunen–Loève expansion a certain realization of such a field can be presented in the eigenfunction ψ_k basis as

$$f(\mathbf{r}) = \sum_{k=1}^n \psi_k(\mathbf{r}) \chi_k \quad (5)$$

with independent variables χ_k normally distributed with probability density

$$\rho_k = \frac{1}{\sqrt{2\pi\lambda_k}} e^{-\frac{\chi_k^2}{2\lambda_k}} \quad \forall k \in 1, \dots, n \quad (6)$$

As stated earlier, ψ_k are the eigenfunctions of the correlation matrix \hat{G}_2 and λ_k are their eigenvalues.

$$\hat{G}_2 \psi_k = \lambda_k \psi_k \quad \forall k \in 1, \dots, n \quad (7)$$

The joint probability density of the whole realization $\boldsymbol{\chi} = (\chi_1, \dots, \chi_n)$ in this orthogonal space of eigenfunctions ψ_k is now the product of independent probability densities for χ_k

$$\rho(\boldsymbol{\chi}) = \prod_{k=1}^n \rho_k(\chi_k, \lambda_k) \quad (8)$$

2.2. A Random Field with an Uncertainty of the Correlation Function

Since the joint probability density (8) depends on the eigenvalues λ_k it changes when the correlation matrix is perturbed. In this section, we use perturbation theory to modify the expression (8) regardless of the stochastic nature of the perturbation \hat{U} of the correlation matrix [84, 85] Further, we will take into account the explicit form of this perturbation in section 2.3.

The perturbed correlation function $G_2(\mathbf{x}) + U(\mathbf{x})$ corresponds to the correlation matrix $\hat{G}_2 + \hat{U}$ with eigenvectors ϕ_k and eigenvalues β_k

$$[\hat{G}_2 + \hat{U}] \phi_k = \beta_k \phi_k \quad \forall k \in 1, \dots, n \quad (9)$$

The modified eigenvalues $\beta_k = \lambda_k + \lambda_{k,1} + \lambda_{k,2}$ now include first- and second-order corrections [85]:

$$\begin{aligned}\lambda_{k,1} &= P_{kk} \\ \lambda_{k,2} &= \sum_{m \neq k} \frac{P_{km}P_{mk}}{\lambda_k - \lambda_m}\end{aligned}\tag{10}$$

where the matrix element P_{km} can be considered as a representation of \hat{U} in the basis set ψ_k

$$P_{km} = (\psi^k, \hat{U}\psi^m) = \sum_{i,j} \psi_i^k \hat{U}_{ij} \psi_j^m \tag{11}$$

The probability density perturbation can be estimated using the second-order Taylor expansion w.r.t perturbation \hat{U}

$$\begin{aligned}\rho_k(\chi_k|\hat{G} + \hat{U}) &= \frac{1}{\sqrt{2\pi(\lambda_k + \lambda_{k,1} + \lambda_{k,2})}} \exp\left[-\frac{\chi_k^2}{2(\lambda_k + \lambda_{k,1} + \lambda_{k,2})}\right] = \\ &= \rho_k(\chi_k, \lambda_k) (1 + f_k(\chi_k, \hat{U}))\end{aligned}\tag{12}$$

The correction $f_k = A(\hat{U}) + B(\hat{U})\chi_k^2 + C(\hat{U})\chi_k^4$ is a quadratic polynomial of χ_k^2 . The coefficients A , B and C contain terms of the first and second order on perturbation \hat{U} (since eigenvalue corrections functionally depend on \hat{U})

$$\begin{aligned}A &= \frac{1}{\lambda_k} \left(-\frac{1}{2}\lambda_{k,1} - \frac{1}{2}\lambda_{k,2} + \frac{3}{8}\lambda_{k,1}^2 \right) \\ B &= \frac{1}{2\lambda_k^2} \left(\lambda_{k,1} + \lambda_{k,2} - \frac{3}{2}\lambda_{k,1}^2 \right) \\ C &= \frac{1}{8\lambda_k^3} \lambda_{k,1}^2\end{aligned}\tag{13}$$

We give a detailed evaluation of the probability density and even expressions for coefficients A , B and C in Appendix A. From this point on, we denote $\rho_k(\chi_k|\hat{G}_2 + \hat{U})$ as $\rho_k(\chi_k|\hat{U})$ for simplicity and bear in mind that this corresponds to a certain \hat{G}_2 . Thus conditional joint probability density for the whole set of χ_i now contains the corrections f_k

$$\rho(\chi|\hat{U}) = \prod_{k=1}^n \rho_k(\chi_k, \lambda_k) (1 + f_k(\chi_k, \hat{U})) \tag{14}$$

2.3. Excess Shannon Entropy

In the section 2.2 we derived the joint probability density independently of the random nature of the perturbation \hat{U} . In this section, we impose a number of conditions on the perturbation and evaluate an expression for Shannon entropy of the field with a perturbed correlation matrix for the certain probability model. Starting from the unperturbed Shannon entropy [74]

$$H_0 = - \int d\chi \sum_i \ln(\rho_i) \prod_k \rho_k \quad (15)$$

one may obtain the expected known result for Gaussian multivariate entropy:

$$H_0 = - \sum_i \int d\chi_i \rho_i \ln(\rho_i) = \frac{1}{2} \ln [(2\pi e)^n \det(\hat{G}_2)] \quad (16)$$

Now we move to perturbed conditional distribution and make several assumptions that allow us to obtain an analytical result for the entropy of such a stochastic perturbation \hat{U} . First, we assume that the perturbation has a zero mean, and its variance is a smooth function $u(x)$. Different realisations of perturbation are completely uncorrelated (see figure 1)

$$\begin{aligned} \mathbb{E}[U(x)] &= 0 \\ \langle U(x)U(x+\tau) \rangle &= u(x)\delta(\tau) \end{aligned} \quad (17)$$

Slight perturbations of correlation function leads to slight perturbation of resulting field which results in loss of information content. Now we express the change of Shannon entropy due to perturbation of correlation function.

The expression for the perturbed Shannon entropy is defined as

$$\begin{aligned} H &= -\mathbb{E}_\chi \ln \langle \rho(\chi|\hat{G}_2 + \hat{U}) \rangle_{\hat{U}} = \\ &= - \int d\chi \int \rho(\chi|\hat{G}_2 + \hat{U}) \rho(\hat{U}) d\hat{U} \ln \left(\int \rho(\chi|\hat{G}_2 + \hat{U}) \rho(\hat{U}) d\hat{U} \right) \end{aligned} \quad (18)$$

We integrate the conditional probability density over various realizations $U(x)$ of perturbation leading to probability density no longer depends on a certain realization of perturbation. We take only terms up to second order

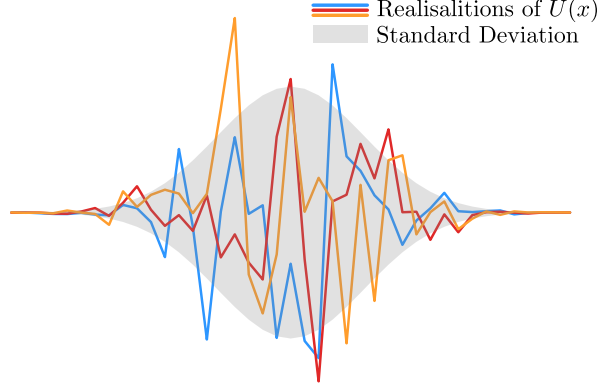


Figure 1: Three different realizations of the perturbation $U(x)$ from the distribution with zero mean and smooth variance.

of perturbations:

$$\begin{aligned}
 \int \rho(\chi|\hat{U})\rho(\hat{U})d\hat{U} &= \langle \prod_k \rho_k (1 + f_k) \rangle_{\hat{U}} = \left\langle 1 + \sum_i f_i + \frac{1}{2} \sum_{i \neq j} f_i f_j \right\rangle_{\hat{U}} \prod_k \rho_k = \\
 &= \left(1 + \sum_i \tilde{f}_i + \frac{1}{2} \sum_{i \neq j} \langle f_i f_j \rangle_{\hat{U}} \right) \prod_k \rho_k
 \end{aligned} \tag{19}$$

Let us denote

$$\tilde{f}_i = \langle f_i \rangle_{\hat{U}} = \langle A + B\chi_i^2 + C\chi_i^4 \rangle_{\hat{U}} = \langle A \rangle_{\hat{U}} + \langle B \rangle_{\hat{U}} \chi_i^2 + \langle C \rangle_{\hat{U}} \chi_i^4 \tag{20}$$

The logarithm of the probability density from (18) averaged over \hat{U} also contains the above-mentioned corrections \tilde{f}_i and $\sum_{i \neq j} \langle f_i f_j \rangle_{\hat{U}}$

$$\ln \langle \rho(\chi, \hat{U}) \rangle_{\hat{U}} = \sum_k \ln \rho_k + \sum_i \tilde{f}_i + \sum_{i \neq j} \langle f_i f_j \rangle_{\hat{U}} \tag{21}$$

Now we can obtain the expression for the perturbed entropy (18) using

(19, 21)

$$\begin{aligned}
H = - \int d\chi \prod_k \rho_k \left(1 + \sum_i \tilde{f}_i + \sum_{i \neq j} \langle f_i f_j \rangle_{\hat{U}} \right) & \left(\sum_j \ln(\rho_j) + \sum_l \tilde{f}_j \right. \\
& \left. + \sum_{i \neq j} \langle f_i f_j \rangle_{\hat{U}} \right) = \\
& = H_0 + H_1 + H_2
\end{aligned} \tag{22}$$

We group the terms containing \tilde{f}_i and $\langle f_i f_j \rangle_{\hat{U}}$ into the summands H_1 and H_2 , respectively

$$H_1 = - \int d\chi \sum_i \tilde{f}_i \prod_k \rho_k - \int d\chi \sum_i \ln(\rho_i) \sum_j \tilde{f}_j \prod_k \rho_k \tag{23}$$

$$H_2 = - \int d\chi \sum_{i \neq j} \langle f_i f_j \rangle_{\hat{U}} \prod_k \rho_k - \int d\chi \sum_i \ln(\rho_i) \sum_{i \neq j} \langle f_i f_j \rangle_{\hat{U}} \prod_k \rho_k \tag{24}$$

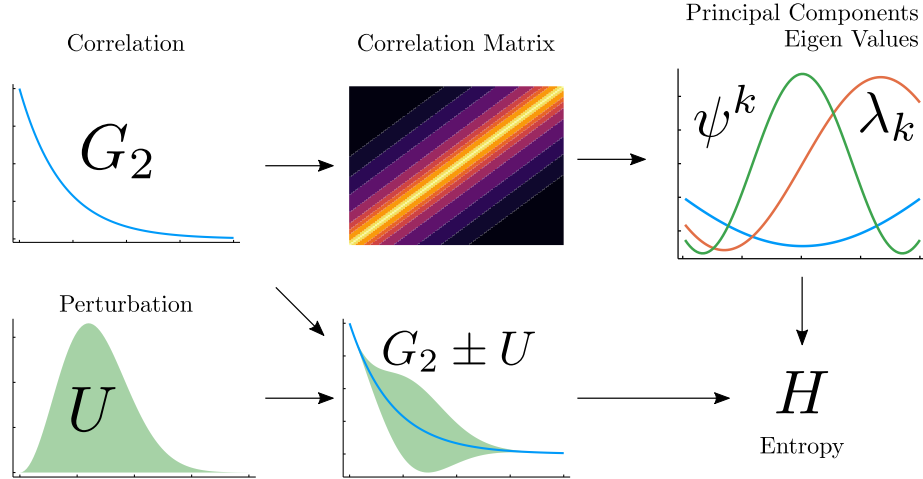


Figure 2: Stages of entropy calculation: calculate eigenvectors and principal components of correlation matrix for certain autocorrelation function, obtain entropy value for certain perturbation

The terms containing $\tilde{f}_i \tilde{f}_j$, $\tilde{f}_k \langle f_i f_j \rangle_{\hat{U}}$, $\langle f_i f_j \rangle_{\hat{U}} \langle f_k f_l \rangle_{\hat{U}}$ are fourth-order infinitesimals, so we neglect them. The final expression for entropy is as follows

$$H = H_0 + \frac{1}{2} \sum_k \left(\frac{\langle \lambda_{k,1} \rangle_{\hat{U}}}{\lambda_k} + \frac{\langle \lambda_{k,2} \rangle_{\hat{U}}}{\lambda_k} \right) \tag{25}$$

Thus, the change in entropy with a small perturbation of the correlation function is (see Figure 2 for schematic illustration):

$$\Delta H = H - H_0 = \sum_{k,m} \frac{1}{2\lambda_k(\lambda_k - \lambda_m)} \sum_{l,n} (\psi_l^k)^2 u_{ln} (\psi_n^m)^2 \quad (26)$$

Evaluation of the previous expression is technically complex so we give detailed calculations in Appendix B. There we also show that H_2 does not contribute to entropy.

2.4. Computational Workflow and Model Application

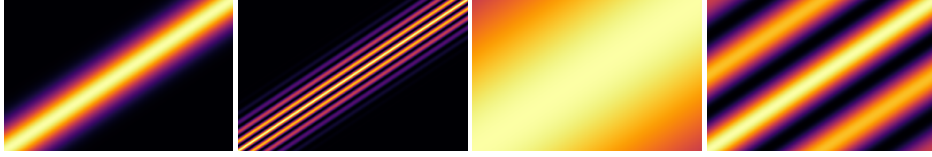
We utilize the following workflow (Figure 2) to illustrate our analytical expression for entropy. First, we compute the correlation matrix based on the given correlation function of the Gaussian field. Then, using singular value decomposition [86] we obtain a set of eigenvalues and eigenvectors for the correlation matrix G_2 . Finally, we apply the expression (26) to calculate the desired additional entropy. We apply this procedure to Gaussian correlation functions of two different widths and to cosine modulated Gaussian functions (Figure 3b). The corresponding correlation matrices are shown in the Figure 3a and Figure 3c shows first three principal components ψ^k of these matrices. They are in a way similar to harmonic functions and follow a certain trend - more "narrow" G_2 is, the ψ^k oscillates more frequently.

2.5. Entropy Analysis with Several Uncertainty Models

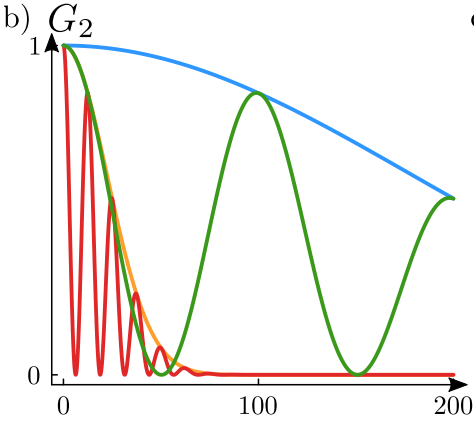
To analyse the proposed model we consider four different parameterized perturbations and study the entropy behaviour depending on their parameters (Figure 4). When choosing these specific forms of perturbation, we proceeded from the following principles. Firstly, an arbitrary function of interest to us from a practical point of view can be represented as a decomposition with respect to the presented elementary perturbations. Also these elementary functions allow us to consider the influence of the perturbation of the original correlation function G_2 in different spatial ranges, both individually and in combination. Thus we analyze the following perturbations:

- The first perturbation is a smooth step-like function with increasing front in the horizontal coordinate p_1 . We can treat it as $U_1(x - p_1)$.
- The second perturbation $U_2(\frac{x-x_0}{p_2})$ is a Gaussian function with a varying width p_2 but a fixed peak position and area under curve

a)



b)



c)

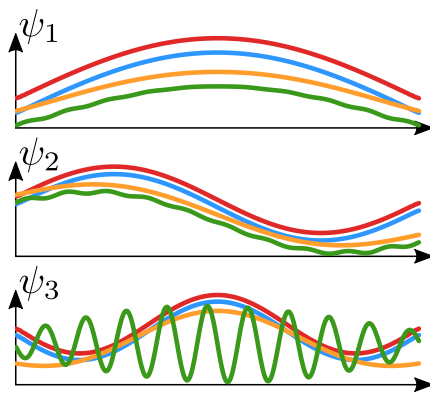


Figure 3: a) correlation matrices; b) Monotonous and oscillating correlation functions; c) Principal components of correlation matrices. Color characterizes one from four correlation functions

- The third perturbation has a form of $F(x) = x^4 e^{-\frac{x^2}{2\sigma^2}}$ and is displaced by p_3 to the right $U_3(x) = F(x - p_3)$
- The fourth perturbation $U_4(x) = F\left(\frac{x}{p_4}\right)$ is similar to the third one but we stretch it in the horizontal direction instead of simple moving.

3. Results and Discussion

In the above mentioned four cases the orders of magnitude of entropy differ, since the principal components vary for different correlation functions. For this reason we normalize the entropy change by its maximum value only for the convenience of visual analysis.

We expect the entropy as a measure of information content to be higher when the perturbation has a more significant impact on the most meaningful regions in G_2 . The initial slope of G_2 and the nearby surroundings appear to be such a region. The figure 4 shows the entropy change normalized by its maximum value for each of proposed perturbations. We make a few nontrivial observations from these graphs. For all types of the correlation functions the less the perturbed region of G_2 , the less entropy is. Moreover, we see that (as expected) the information content of the different regions is not the same.

Moving the front of perturbation to the right in the sub-figure 4.a decreases the perturbation in the region close to zero shift which results in decreasing the entropy. On the contrary, widening the perturbation in the case 4.b increases the perturbation in the region close to zero shift and decreases the entropy change. Thus, the change of entropy increases with increasing the perturbation in the region close to zero shift. It means that, as we expected, the information content of this region is higher. The sub-figure 4.c shows a nontrivial oscillation over existing trend for the green curve which corresponds to the period of the green G_2 oscillation. As for the case 4.d we can notice that the entropy first increases and then decreases, because the perturbation, on the one hand, increases its area but, on the other hand, moves out of the region of interest.

Thus, the analysis of the developed model on simple functions confirms our qualitative expectations of entropy for random fields. However, the main advantage of the model is its simplicity for numerical calculations. In the next section, we will try to estimate the complexity of calculating the entropy for proposed model uncertainty.

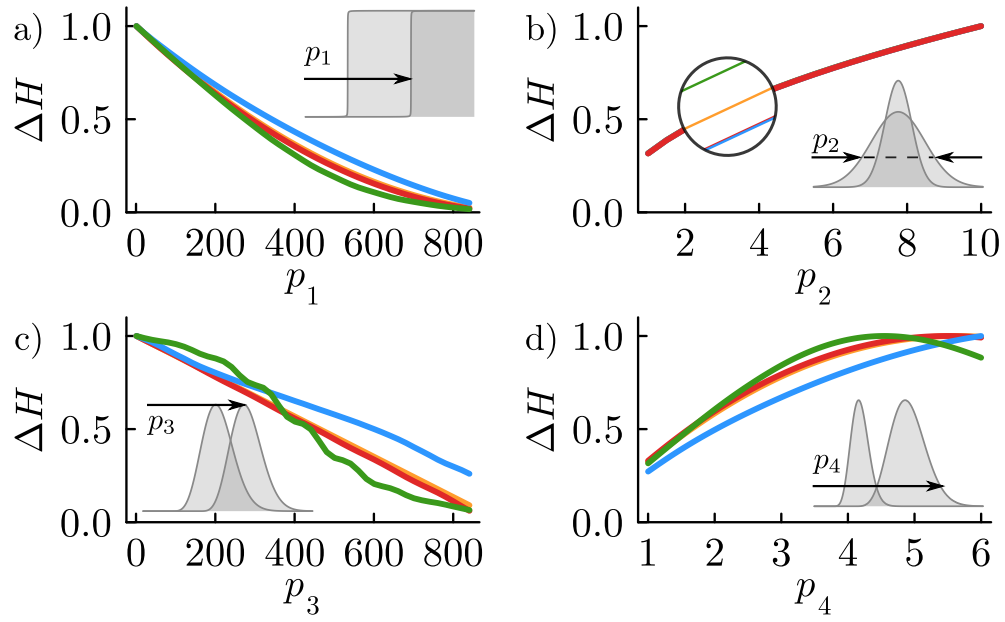


Figure 4: The entropy change with different correlation functions and different perturbations normalized by the maximum value. The gray insets show the form of perturbation: a) moving step, b) widening Gaussian, c) moving and d) widening bell-like functions. Color marks the same correlation functions as shown in figure 3. In the case b) the plots are distinguishable only upon closer look.

3.1. Information Content of Heterogeneous Media Descriptors

Our results are of particular interest in the field of porous materials research, since the statistical characterisation of heterogeneous random media is based on the use of correlation functions [23]. Two-phase random media can be characterised with an indicator function

$$I(\mathbf{r}) = \begin{cases} 1, & \text{if } \mathbf{r} \text{ is solid} \\ 0, & \text{otherwise} \end{cases} \quad (27)$$

and the indicator function of its inter-phase boundary is defined as follows [23]:

$$M(\mathbf{r}) = |\nabla I(\mathbf{r})| \quad (28)$$

Thus the n-point function (here brackets define ensemble average over realizations):

$$S_n(\mathbf{r}_1 \dots \mathbf{r}_n) = \langle I(\mathbf{r}_1) \dots I(\mathbf{r}_n) \rangle \quad (29)$$

has the sense of probability for certain phase of random media to exist in points $\mathbf{r}_1 \dots \mathbf{r}_n$ at the same time. Furthermore, surface-volume and surface-surface functions can be used to statistically characterise interposition between surface and volume and surface itself.

$$F_{sv}(\mathbf{r}_1, \mathbf{r}_2) = \langle M(\mathbf{r}_1)I(\mathbf{r}_2) \rangle \quad (30)$$

$$F_{ss}(\mathbf{r}_1, \mathbf{r}_2) = \langle M(\mathbf{r}_1)M(\mathbf{r}_2) \rangle \quad (31)$$

These and other so called descriptor functions are the important tool for characterisation and stochastic reconstruction of heterogeneous porous geometry. Even more complex correlations of solid, interface and other regions can be used. For example [87] suggest a robust way to calculate the n-point surface-surface correlation functions for a wide variety of cases.

Quite often characterisation should be done repeatedly as a part of an optimization process. This happens, for example, when solving inverse problem of porous media reconstruction [88, 89, 90, 54, 91] with initially given statistical or any other properties. In this case execution speed of a single characterization procedure governs the execution speed of the whole algorithm. Fast Fourier Transform [92] is a powerful tool to accelerate any correlation-based statistical descriptor which becomes a significant advantage when choosing

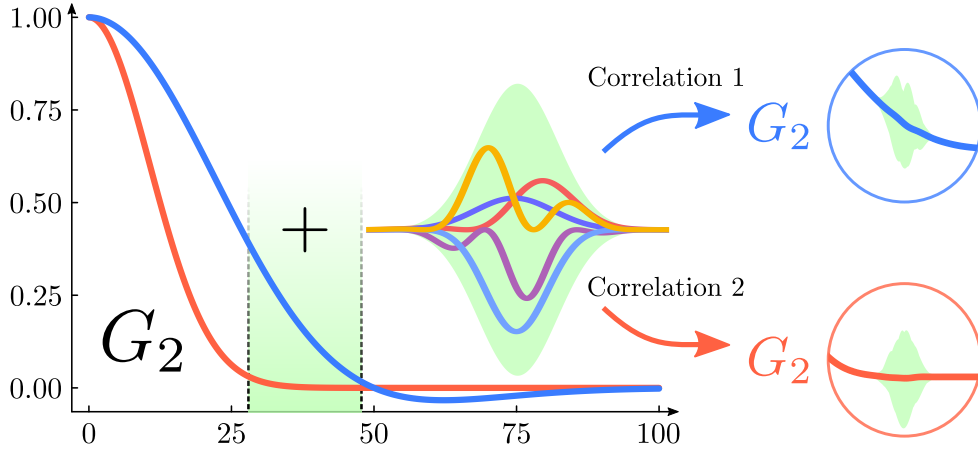


Figure 5: Perturbations from the same distribution are in different degree crucial for thick and thin correlation. Repeated sampling such perturbation together with direct reconstruction is a way to estimate the scatter of S_2 and F_{ss} for resulting binary images

the set of descriptors for certain problem. Thus the information content of different descriptor functions expressed in terms of Shannon entropy is a way to choose the most informative and computationally effective one for certain type of porous media structure.

To illustrate how perturbation correlation function G_2 influences solid-solid S_2 and surface-surface F_{ss} correlation functions we perform the following numerical experiment (Figure 5). For given thick correlation function 1 which is cosine modulated by Gaussian and thin correlation function 2 which is just a decreasing Gaussian we perform a series of perturbations. Each perturbation is space and amplitude limited smooth oscillating curve (in contrast to non-correlated noise in our model). The perturbation is localised in such a region that is more meaningful for thick correlation rather than for the thin one. Then we use approach given in [88] to generate a series of reconstructions. In particular, for each perturbed G_2 we obtain its spectral density and generate Gaussian random field using set of random but permanent for each perturbation spectral coefficients. The operation is fully equivalent to convolving certain realization of white noise with kernel which correlation equals correlation of desired field (Figure 6). Truncating this field at certain level produces binary structures (Figure 7) with slightly perturbed S_2 and F_{ss} which now have the shape of clouds not single curves (Figure 8). When equally perturbing regions of different meaningfulness of different correla-

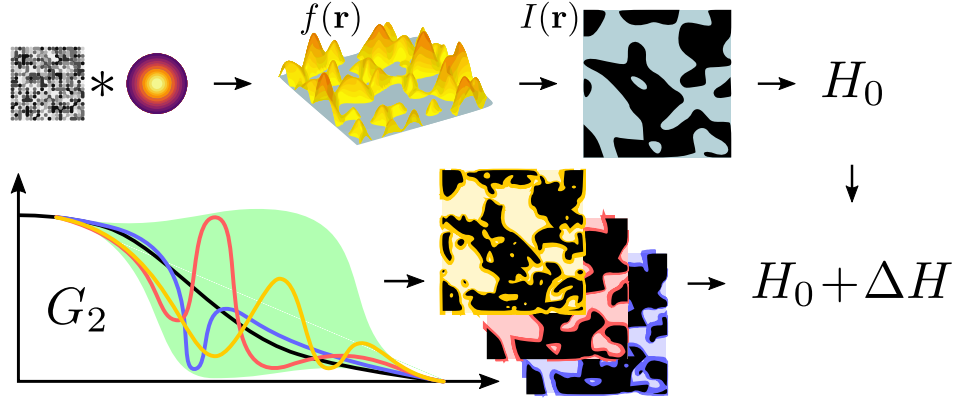


Figure 6: Random noise convolved with creating perturbation of correlation function G_2 produces certain realization of random field $f(\mathbf{r})$. When thresholded at certain level the field becomes binary $I(\mathbf{r})$. Slight perturbations of correlation function leads to slight perturbation of resulting field which results in degeneracy of field and loss of information content

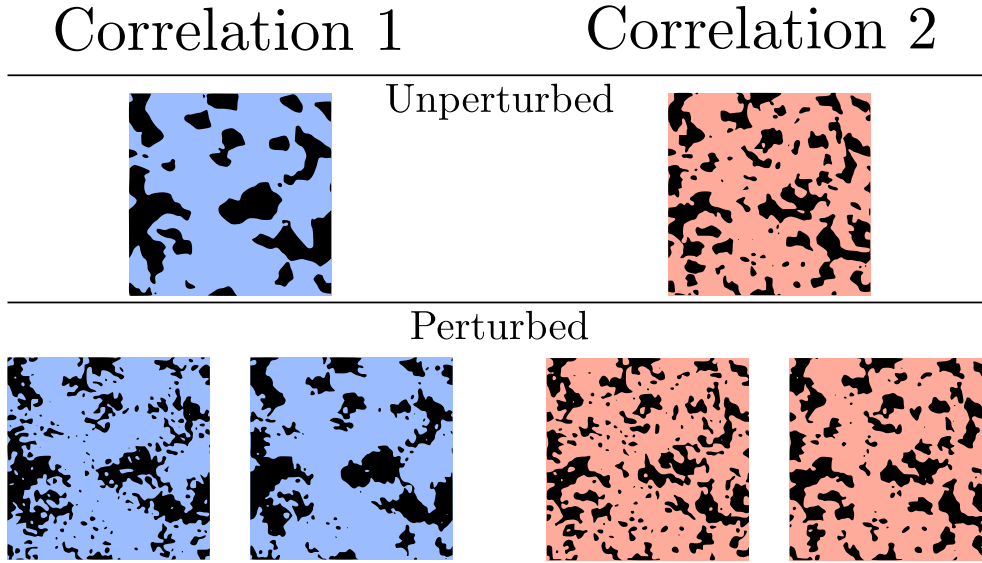


Figure 7: Results of generating binary random media with same initial noise for both thick and thin correlations 1 and 2, respectively. Top: unperturbed correlations, bottom: perturbed correlations

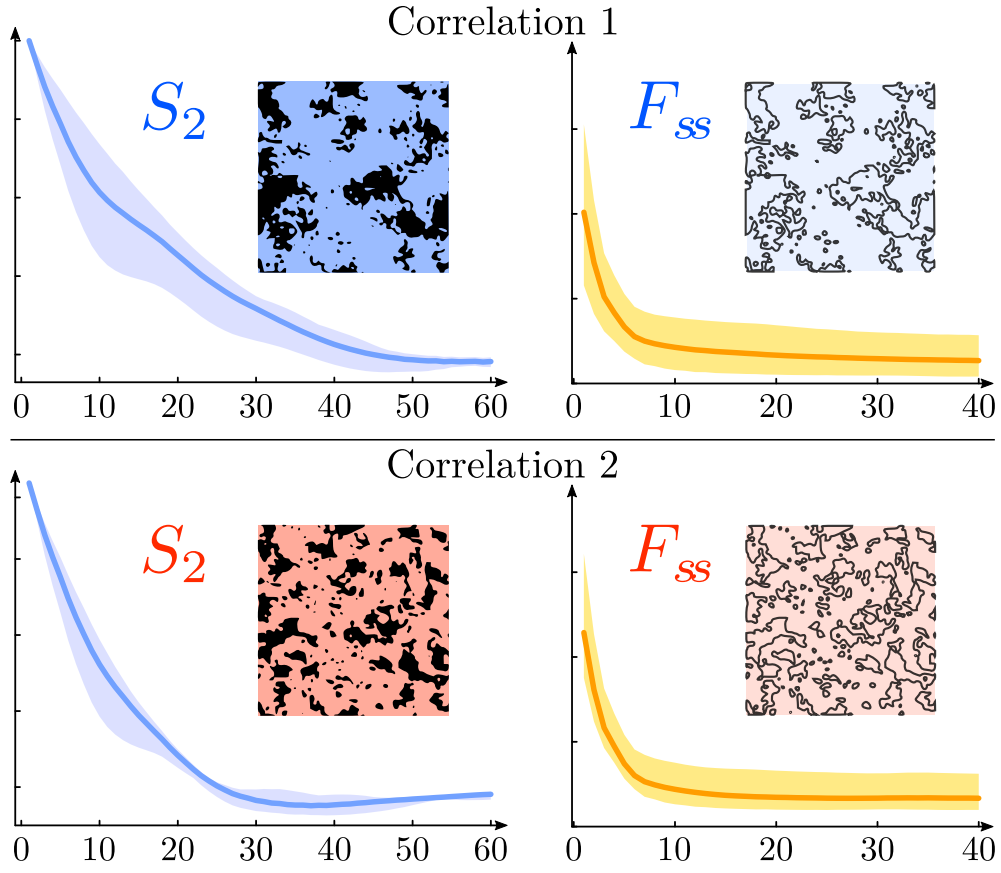


Figure 8: S_2 and F_{ss} correlation function clouds for equally perturbed thick and thin correlations 1, 2 respectively (Figure 5). Perturbation of more meaningful regions of correlation function produces wider clouds for S_2 and F_{ss}

tion functions the disturbed thicker correlation produces wider clouds both for S_2 and F_{ss} . This result well coincides with the idea that perturbation of more meaningful region leads to higher impact not only on entropy but also on different descriptors. The developed approach allows us to estimate the information content of correlation-based descriptors and bridges the gap between information theory and heterogeneous media reconstruction. Thus, our theoretical result can be applied in further research on the topic which is of great interest.

3.2. Computational Cost of Monte Carlo Entropy Calculations with Model Uncertainty

Monte Carlo sampling is an alternate and commonly used way of the numerical calculation of integrals e. g. the one for entropy. To calculate the integral of two functions product f and ρ (where ρ defines some probability distribution) using MC one can approximate it with the finite sum of function values $f(x_i)$ at the points x_i sampled from the probability density $\rho(x_i)$

$$\int f(x)\rho(x)dx \approx \frac{1}{N} \sum_{i=1}^N f(x_i) \quad (32)$$

The entropy can be obtained by the integral (18)

$$H = - \int dU \pi(U) \int d\chi \rho(\chi|U) \ln \left[\int dS \rho(\chi|S) \pi(S) \right] \quad (33)$$

where $\pi(U)$ is the probability density of the perturbation U while $\rho(\chi|U)$ is the conditional probability of χ in the case of this perturbation. To calculate this integral we need to consequently apply Monte Carlo sampling for calculation of all the internal integrals. Their order is conditioned by the sampling convenience. The outer Monte Carlo sum

$$\frac{1}{N} \sum_{i=1}^N f(U_i) \quad U_i \in \pi(U) \quad (34)$$

requires the calculation of the medium sum

$$f(U_i) = \frac{1}{K} \sum_{j=1}^K g(\chi_j) \quad \chi_j \in \rho(\chi|U_i) \quad (35)$$

which again requires the precalculation of

$$g(\chi_j) = \ln \left[\int dS \pi(S) \rho(\chi_j|S) \right] = \ln \left[\frac{1}{M} \sum_{k=1}^M \rho(\chi_j|S_k) \right] \quad S_k \in \pi(S) \quad (36)$$

The whole algorithm seems to be extremely computationally expensive. Genuinely, even for a simple case of 5×5 matrix Monte Carlo summation should be done in the 10-dimensional space ($5 \times (5 - 1)/2$ different variables) with $N \approx M \approx K \approx 10^{10}$ summands.

Moreover, the expressions (35, 36) require K and M calculations of ρ_k which is a complex procedure itself. Actually, singular value decomposition of the correlation matrix should be done $K \times N$ times. These estimations altogether allow us to state with complete confidence that direct Monte Carlo calculation of the entropy of Gaussian field with random correlation matrix perturbation is not so easy to obtain in reasonable time and analytical models are highly desirable.

Monte-Carlo-based entropic approach for information content was presented in [26]. The authors introduced energy landscape as a distance functional between certain S_2 functions in configuration space. They also performed Monte-Carlo sampling to obtain these landscapes for different patterns. This resulted in approximate estimate of related to entropy self-information via the energy landscape profile. This approach in terms of information content was used to characterize the degeneracy of different structures like single and hard disks, Poisson point processes and polycrystals. The analytical framework, as presented in this work, attacks the problem from a completely different angle and potentially allows to obtain information content for any 2D or 3D image without both Monte-Carlo simulation and estimations from relationships obtained with such simulations from small-scale 2D images.

4. Summary and outlook

This research paper presents a theoretical framework aimed at evaluating the information content of descriptors employed in the characterization and reconstruction of structures within random fields. Specifically, our focus lies on quantifying the information loss arising from model uncertainty during the reconstruction process. We substantiate our claim by demonstrating that stochastic perturbations introduced into the correlation function of random fields result in a decrease in their information content.

In this work, we develop a theoretical model that considers Gaussian fields possessing an arbitrary correlation matrix. Leveraging the Karhunen-Loève transform and matrix perturbation theory, we derive an analytical expression for the Shannon entropy of the perturbed random fields. Additionally, we ascertain that distinct regions of the correlation function exhibit varying levels of informativeness and sensitivity to perturbations. To exemplify the application of the analytical expression for entropy calculation, we outline a computational workflow within the paper. We explore several uncertainty models, each incorporating different parameterized perturbations, and analyze the behavior of entropy for each perturbation. This analysis reveals that the information content is more pronounced in regions where the perturbation exerts a significant impact on the correlation function.

The findings of this study bear significance on the characterization and reconstruction of heterogeneous media, particularly within the domain of porous materials research. The utilization of correlation functions as descriptors for statistical characterization is a common practice within this field. Our proposed model offers a means to estimate the information content associated with such descriptors, thereby facilitating the selection of the most informative ones.

Moreover, it is noteworthy to delineate several prospective avenues for the advancement of the developed model as well as its practical applications:

- **Generalization to Non-Gaussian Fields:** the current model assumes Gaussian random fields. Exploring the information content and entropy analysis for non-Gaussian fields would be an interesting direction for further research. Many real-world structures exhibit non-Gaussian behavior, and understanding the impact of non-Gaussianity on the information content of descriptors could lead to more accurate characterization and reconstruction methods.
- **Application to Specific Fields:** The framework presented in this research has wide applicability in various fields involving the characterization of structures. Future studies could focus on specific applications, such as material science, geophysics, or biomedical imaging. Tailoring the framework to the unique challenges and requirements of these fields would provide domain-specific insights and contribute to advancements in those areas.
- **Integration with Machine Learning Techniques:** Integrating the pro-

posed framework with machine learning techniques could lead to enhanced information content assessment and reconstruction capabilities. Exploring the use of deep learning models for automatic feature extraction and optimization of reconstruction algorithms based on the estimated information content could improve the overall performance and efficiency of the framework.

- **Real-Time Information Content Assessment:** Investigating real-time information content assessment methods could be valuable in dynamic systems where structures evolve or change over time. Developing algorithms that can continuously monitor the information content of descriptors and adaptively adjust reconstruction processes based on changing structures would be a significant advancement.
- **Comparative Analysis of Descriptors:** Conducting a comparative analysis of different descriptors commonly used in structure characterization could provide insights into their relative information content and effectiveness. Such an analysis would help researchers choose the most informative and suitable descriptors for specific applications, optimizing the trade-off between computational cost and accuracy.

By pursuing these research advances and improvements, the proposed framework can be further refined, validated, and applied to a wider range of real-world scenarios. Overall, this research contributes to bridging the gap between descriptor-based heterogeneous media reconstruction and information theory. The developed analytical framework offers a computationally effective way to assess the information content of descriptors applied to arbitrary structures. The theoretical results presented in this paper can be further applied in related research areas and provide valuable insights for the optimization of reconstruction algorithms in porous media and other fields.

5. Acknowledgements

This research was supported by the Russian Science Foundation grant 23-74-00069. Collaborative effort of the authors is within the FaT iMP (Flow and Transport in Media with Pores) research group (www.porenetwork.com). We thank Dr. Konstantin Abrosimov for suggestions and administrative work. We express sincere gratitude to our colleagues Dr. Nikolay Evstigneev and Dr. Oleg Ryabkov for fruitful discussions and comments on this work.

References

- [1] V. Springel, C. S. Frenk, S. D. White, The large-scale structure of the universe, *nature* 440 (7088) (2006) 1137–1144.
- [2] P. F. Hopkins, A new class of accurate, mesh-free hydrodynamic simulation methods, *Monthly Notices of the Royal Astronomical Society* 450 (1) (2015) 53–110.
- [3] V. Balashov, Dissipative spatial discretization of a phase field model of multiphase multicomponent isothermal fluid flow, *Computers & Mathematics with Applications* 90 (2021) 112–124.
- [4] O. Rozenbaum, S. R. du Roscoat, Representative elementary volume assessment of three-dimensional x-ray microtomography images of heterogeneous materials: Application to limestones, *Physical Review E* 89 (5) (2014) 053304.
- [5] M. V. Karsanina, K. M. Gerke, E. B. Skvortsova, D. Mallants, Universal spatial correlation functions for describing and reconstructing soil microstructure, *PloS one* 10 (5) (2015) e0126515.
- [6] R. Ledesma-Alonso, R. Barbosa, J. Ortegón, Effect of the image resolution on the statistical descriptors of heterogeneous media, *Physical Review E* 97 (2) (2018) 023304.
- [7] H. Chen, X. He, Q. Teng, R. E. Sheriff, J. Feng, S. Xiong, Super-resolution of real-world rock microcomputed tomography images using cycle-consistent generative adversarial networks, *Physical Review E* 101 (2) (2020) 023305.
- [8] D. Prokhorov, V. Lisitsa, Y. Bazaikin, Digital image reduction for the analysis of topological changes in the pore space of rock matrix, *Computers and Geotechnics* 136 (2021) 104171.
- [9] A. Derossi, K. M. Gerke, M. V. Karsanina, B. Nicolai, P. Verboven, C. Severini, Mimicking 3d food microstructure using limited statistical information from 2d cross-sectional image, *Journal of food engineering* 241 (2019) 116–126.

- [10] A. Nagdalian, I. Rzhepakovsky, S. Siddiqui, S. Piskov, N. Oboturova, L. Timchenko, A. Lodygin, A. Blinov, S. Ibrahim, Analysis of the content of mechanically separated poultry meat in sausage using computing microtomography, *Journal of Food Composition and Analysis* 100 (2021) 103918.
- [11] S. Park, S. Lim, P. Siriviriyakul, J. S. Jeon, Three-dimensional pore network characterization of reconstructed extracellular matrix, *Physical Review E* 101 (5) (2020) 052414.
- [12] M. Garum, P. W. Glover, P. Lorinczi, R. Drummond-Brydson, A. Hassanpour, Micro-and nano-scale pore structure in gas shale using x μ -ct and fib-sem techniques, *Energy & Fuels* 34 (10) (2020) 12340–12353.
- [13] K. M. Gerke, E. V. Korostilev, K. A. Romanenko, M. V. Karsanina, Going submicron in the precise analysis of soil structure: A fib-sem imaging study at nanoscale, *Geoderma* 383 (2021) 114739.
- [14] P. F. Hopkins, Why do stars form in clusters? an analytic model for stellar correlation functions, *Monthly Notices of the Royal Astronomical Society* 428 (3) (2013) 1950–1957.
- [15] Y. Jiao, E. Padilla, N. Chawla, Modeling and predicting microstructure evolution in lead/tin alloy via correlation functions and stochastic material reconstruction, *Acta Materialia* 61 (9) (2013) 3370–3377.
- [16] D. S. Fomin, A. V. Yudina, K. A. Romanenko, K. N. Abrosimov, M. V. Karsanina, K. M. Gerke, Soil pore structure dynamics under steady-state wetting-drying cycle, *Geoderma* 432 (2023) 116401.
- [17] K. M. Gerke, M. V. Karsanina, R. Katsman, Calculation of tensorial flow properties on pore level: Exploring the influence of boundary conditions on the permeability of three-dimensional stochastic reconstructions, *Physical Review E* 100 (5) (2019) 053312.
- [18] A. Róžański, J. Rainer, D. Stefaniuk, I. Sevostianov, D. Łydzba, Identification of ‘replacement’ microstructure for porous medium from thermal conductivity measurements: Problem formulation and numerical solution, *International Journal of Engineering Science* 182 (2023) 103788.

- [19] B. H. Zimm, The scattering of light and the radial distribution function of high polymer solutions, *The Journal of chemical physics* 16 (12) (1948) 1093–1099.
- [20] N. Becker, A. Rosa, R. Everaers, The radial distribution function of worm-like chains, *The European Physical Journal E* 32 (2010) 53–69.
- [21] H.-J. Vogel, U. Weller, S. Schlüter, Quantification of soil structure based on minkowski functions, *Computers & Geosciences* 36 (10) (2010) 1236–1245.
- [22] G. E. Schröder-Turk, W. Mickel, S. C. Kapfer, M. A. Klatt, F. M. Schaller, M. J. Hoffmann, N. Kleppmann, P. Armstrong, A. Inayat, D. Hug, et al., Minkowski tensor shape analysis of cellular, granular and porous structures, *Advanced Materials* 23 (22-23) (2011) 2535–2553.
- [23] S. Torquato, *Random heterogeneous materials: microstructure and macroscopic properties*, Springer-Verlag New York, 2002. doi:10.1007/978-1-4757-6355-3.
- [24] H.-J. Vogel, M. Balseiro-Romero, A. Kravchenko, W. Otten, V. Pot, S. Schlüter, U. Weller, P. C. Baveye, A holistic perspective on soil architecture is needed as a key to soil functions, *European Journal of Soil Science* 73 (1) (2022) e13152.
- [25] A. Yudina, Y. Kuzyakov, Dual nature of soil structure: The unity of aggregates and pores, *Geoderma* 434 (2023) 116478.
- [26] C. J. Gommers, Y. Jiao, S. Torquato, Microstructural degeneracy associated with a two-point correlation function and its information content, *Physical Review E* 85 (5) (2012) 051140.
- [27] A. Nur, G. Mavko, J. Dvorkin, D. Galmudi, Critical porosity: A key to relating physical properties to porosity in rocks, *The Leading Edge* 17 (3) (1998) 357–362.
- [28] R. P. Chapuis, M. Aubertin, On the use of the kozeny carman equation to predict the hydraulic conductivity of soils, *Canadian Geotechnical Journal* 40 (3) (2003) 616–628.

- [29] J. Kozeny, Über kapillare leitung des wassers im boden-aufstieg, versickerung und anwendung auf die bewässerung, sitzungsberichte der akademie der wissenschaften wien, Mathematisch Naturwissenschaftliche Abteilung 136 (1927) 271–306.
- [30] P. C. Carman, Fluid flow through a granular bed, Trans. Inst. Chem. Eng. London 15 (1937) 150–156.
- [31] P. Debye, H. Anderson Jr, H. Brumberger, Scattering by an inhomogeneous solid. ii. the correlation function and its application, Journal of applied Physics 28 (6) (1957) 679–683.
- [32] C. J. Gommès, Stochastic models of disordered mesoporous materials for small-angle scattering analysis and more, Microporous and Mesoporous Materials 257 (2018) 62–78.
- [33] P. Adler, C. G. Jacquin, J. Quiblier, Flow in simulated porous media, International Journal of Multiphase Flow 16 (4) (1990) 691–712.
- [34] K. M. Gerke, M. V. Karsanina, Improving stochastic reconstructions by weighting correlation functions in an objective function, EPL (Europhysics Letters) 111 (5) (2015) 56002.
- [35] P. Čapek, On the importance of simulated annealing algorithms for stochastic reconstruction constrained by low-order microstructural descriptors, Transport in Porous Media 125 (1) (2018) 59–80.
- [36] P. Tahmasebi, M. Sahimi, Cross-correlation function for accurate reconstruction of heterogeneous media, Physical review letters 110 (7) (2013) 078002.
- [37] J. Feng, Q. Teng, X. He, X. Wu, Accelerating multi-point statistics reconstruction method for porous media via deep learning, Acta Materialia 159 (2018) 296–308.
- [38] M. Gravey, G. Mariethoz, Quicksampling v1. 0: a robust and simplified pixel-based multiple-point simulation approach, Geoscientific Model Development 13 (6) (2020) 2611–2630.
- [39] F. Zhang, Q. Teng, X. He, X. Wu, X. Dong, Improved recurrent generative model for reconstructing large-size porous media from two-dimensional images, Physical Review E 106 (2) (2022) 025310.

- [40] D. Volkhonskiy, E. Muravleva, O. Sudakov, D. Orlov, E. Burnaev, D. Koroteev, B. Belozarov, V. Krutko, Generative adversarial networks for reconstruction of three-dimensional porous media from two-dimensional slices, *Physical Review E* 105 (2) (2022) 025304.
- [41] C. Chubb, J. I. Yellott, Every discrete, finite image is uniquely determined by its dipole histogram, *Vision Research* 40 (5) (2000) 485–492.
- [42] D. T. Fullwood, S. R. Niezgod, S. R. Kalidindi, Microstructure reconstructions from 2-point statistics using phase-recovery algorithms, *Acta Materialia* 56 (5) (2008) 942–948.
- [43] S. Dietrich, A. Haase, Scattering of x-rays and neutrons at interfaces, *Physics Reports* 260 (1-2) (1995) 1–138.
- [44] H. Li, S. Singh, N. Chawla, Y. Jiao, Direct extraction of spatial correlation functions from limited x-ray tomography data for microstructural quantification, *Materials Characterization* 140 (2018) 265–274.
- [45] M. V. Karsanina, E. V. Lavrukhin, D. S. Fomin, A. V. Yudina, K. N. Abrosimov, K. M. Gerke, Compressing soil structural information into parameterized correlation functions, *European Journal of Soil Science* 72 (2) (2021) 561–577.
- [46] Y. Jiao, N. Chawla, Modeling and characterizing anisotropic inclusion orientation in heterogeneous material via directional cluster functions and stochastic microstructure reconstruction, *Journal of Applied Physics* 115 (9) (2014) 093511.
- [47] K. M. Gerke, M. V. Karsanina, R. V. Vasilyev, D. Mallants, Improving pattern reconstruction using directional correlation functions, *Europhysics Letters* 106 (6) (2014) 66002.
- [48] J. Yao, P. Frykman, F. Kalaydjian, J. Thovert, P. Adler, High-order moments of the phase function for real and reconstructed model porous media: a comparison, *Journal of colloid and interface science* 156 (2) (1993) 478–490.
- [49] P. Čapek, V. Hejtmánek, J. Kolafa, L. Brabec, Transport properties of stochastically reconstructed porous media with improved pore connectivity, *Transport in porous media* 88 (2011) 87–106.

- [50] M. V. Karsanina, K. M. Gerke, E. B. Skvortsova, A. L. Ivanov, D. Malants, Enhancing image resolution of soils by stochastic multiscale image fusion, *Geoderma* 314 (2018) 138–145.
- [51] A. Adam, F. Wang, X. Li, Efficient reconstruction and validation of heterogeneous microstructures for energy applications, *International Journal of Energy Research* 46 (15) (2022) 22757–22771.
- [52] Y. Jiao, F. Stillinger, S. Torquato, A superior descriptor of random textures and its predictive capacity, *Proceedings of the National Academy of Sciences* 106 (42) (2009) 17634–17639.
- [53] W. R. Campaigne, P. W. Fieguth, Frozen-state hierarchical annealing, *IEEE transactions on image processing* 22 (4) (2012) 1486–1497.
- [54] M. V. Karsanina, K. M. Gerke, Hierarchical optimization: Fast and robust multiscale stochastic reconstructions with rescaled correlation functions, *Physical review letters* 121 (26) (2018) 265501.
- [55] F. Wang, D. P. Landau, Efficient, multiple-range random walk algorithm to calculate the density of states, *Physical review letters* 86 (10) (2001) 2050.
- [56] C. J. Gommers, Y. Jiao, S. Torquato, Density of states for a specified correlation function and the energy landscape, *Physical review letters* 108 (8) (2012) 080601.
- [57] P.-E. Chen, W. Xu, Y. Ren, Y. Jiao, Probing information content of hierarchical n-point polytope functions for quantifying and reconstructing disordered systems, *Physical Review E* 102 (1) (2020) 013305.
- [58] M. Skolnick, S. Torquato, Understanding degeneracy of two-point correlation functions via debye random media, *Physical Review E* 104 (4) (2021) 045306.
- [59] J.-F. Thovert, V. V. Mourzenko, On the influence of boundary conditions when determining transport coefficients from digital images of heterogeneous media., *Advances in Water Resources* 141 (2020) 103612.
- [60] H. Scandelli, A. Ahmadi-Senichault, C. Levet, J. Lachaud, Computation of the permeability tensor of non-periodic anisotropic porous media from 3d images, *Transport in Porous Media* 142 (3) (2022) 669–697.

- [61] H. Chen, X. Wu, M. Han, Y. Zhang, Impacts of solid wall boundary conditions in the lattice boltzmann method on turbulent outdoor flow: A case study of a single 1: 1: 2 building model, *Building and Environment* 226 (2022) 109708.
- [62] D. Zhang, R. Zhang, S. Chen, W. E. Soll, Pore scale study of flow in porous media: Scale dependency, rev, and statistical rev, *Geophysical research letters* 27 (8) (2000) 1195–1198.
- [63] K. M. Gerke, M. V. Karsanina, How pore structure non-stationarity compromises flow properties representativity (rev) for soil samples: Pore-scale modelling and stationarity analysis, *European Journal of Soil Science* 72 (2) (2021) 527–545.
- [64] B. Ghanbarian, Estimating the scale dependence of permeability at pore and core scales: Incorporating effects of porosity and finite size, *Advances in Water Resources* 161 (2022) 104123.
- [65] P. Tahmasebi, M. Sahimi, Reconstruction of nonstationary disordered materials and media: Watershed transform and cross-correlation function, *Physical Review E* 91 (3) (2015) 032401.
- [66] C. J. Gommès, J.-P. Pirard, Morphological models of complex ordered materials based on inhomogeneously clipped gaussian fields, *Physical Review E* 80 (6) (2009) 061401.
- [67] M. V. Karsanina, K. M. Gerke, Stochastic (re) constructions of non-stationary material structures: Using ensemble averaged correlation functions and non-uniform phase distributions, *Physica A: Statistical Mechanics and its Applications* 611 (2023) 128417.
- [68] K. M. Gerke, M. V. Karsanina, D. Mallants, Universal stochastic multiscale image fusion: an example application for shale rock, *Scientific reports* 5 (1) (2015) 1–12.
- [69] J. Havelka, A. Kučerová, J. Šýkora, Compression and reconstruction of random microstructures using accelerated lineal path function, *Computational Materials Science* 122 (2016) 102–117.

- [70] S. Kamrava, P. Tahmasebi, M. Sahimi, Linking morphology of porous media to their macroscopic permeability by deep learning, *Transport in Porous Media* 131 (2) (2020) 427–448.
- [71] M. Röding, Z. Ma, S. Torquato, Predicting permeability via statistical learning on higher-order microstructural information, *Scientific reports* 10 (1) (2020) 1–17.
- [72] S. Cheng, Y. Jiao, Y. Ren, Data-driven learning of 3-point correlation functions as microstructure representations, *Acta Materialia* 229 (2022) 117800.
- [73] E. Lavrukhin, M. Karsanina, K. Gerke, Stochastic reconstruction of particulate media using simulated annealing: improving pore connectivity, *EPL* (2023).
- [74] C. E. Shannon, A mathematical theory of communication, *The Bell system technical journal* 27 (3) (1948) 379–423.
- [75] D. T. Hristopulos, *Random fields for spatial data modeling*, Springer, 2020.
- [76] S. Ma, Y. Dai, Principal component analysis based methods in bioinformatics studies, *Briefings in bioinformatics* 12 (6) (2011) 714–722.
- [77] W. Stacklies, H. Redestig, M. Scholz, D. Walther, J. Selbig, *pcamethods—a bioconductor package providing pca methods for incomplete data*, *Bioinformatics* 23 (9) (2007) 1164–1167.
- [78] S. P. Mishra, U. Sarkar, S. Taraphder, S. Datta, D. Swain, R. Saikhom, S. Panda, M. Laishram, Multivariate statistical data analysis-principal component analysis (pca), *International Journal of Livestock Research* 7 (5) (2017) 60–78.
- [79] S. L. Brunton, J. L. Proctor, J. N. Kutz, Discovering governing equations from data by sparse identification of nonlinear dynamical systems, *Proceedings of the national academy of sciences* 113 (15) (2016) 3932–3937.
- [80] K. Carlberg, Y. Choi, S. Sargsyan, Conservative model reduction for finite-volume models, *Journal of Computational Physics* 371 (2018) 280–314.

- [81] P. Sarma, L. J. Durlofsky, K. Aziz, W. H. Chen, Efficient real-time reservoir management using adjoint-based optimal control and model updating, *Computational Geosciences* 10 (1) (2006) 3.
- [82] M. Elizarev, A. Mukhin, A. Khlyupin, Objective-sensitive principal component analysis for high-dimensional inverse problems, *Computational Geosciences* 25 (2021) 2019–2031.
- [83] I. G. Vladimirov, I. R. Petersen, M. R. James, A quantum karhunen-loeve expansion and quadratic-exponential functionals for linear quantum stochastic systems, in: 2019 IEEE 58th Conference on Decision and Control (CDC), IEEE, 2019, pp. 425–430.
- [84] J. O. Hirschfelder, W. B. Brown, S. T. Epstein, Recent developments in perturbation theory, *Advances in quantum chemistry* 1 (1964) 255–374.
- [85] L. D. Landau, E. M. Lifshitz, *Quantum mechanics: non-relativistic theory*, Vol. 3, Elsevier, 2013.
- [86] G. H. Golub, C. F. Van Loan, *Matrix computations*, JHU press, 2013.
- [87] A. Samarin, V. Postnicov, M. V. Karsanina, E. V. Lavrukhin, D. Gafurova, N. M. Evstigneev, A. Khlyupin, K. M. Gerke, Robust surface-correlation-function evaluation from experimental discrete digital images, *Phys. Rev. E* [accepted] (2023).
- [88] A. P. Roberts, Statistical reconstruction of three-dimensional porous media from two-dimensional images, *Physical Review E* 56 (3) (1997) 3203.
- [89] C. Yeong, S. Torquato, Reconstructing random media, *Physical review E* 57 (1) (1998) 495.
- [90] P. Tahmasebi, M. Sahimi, Reconstruction of three-dimensional porous media using a single thin section, *Physical Review E* 85 (6) (2012) 066709.
- [91] A. Cherkasov, A. Ananev, M. Karsanina, A. Khlyupin, K. Gerke, Adaptive phase-retrieval stochastic reconstruction with correlation functions: Three-dimensional images from two-dimensional cuts, *Physical Review E* 104 (3) (2021) 035304.

- [92] E. O. Brigham, The fast Fourier transform and its applications, Prentice-Hall, Inc., 1988.
- [93] H. Cramér, Mathematical methods of statistics, Vol. 26, Princeton university press, 1999.

Appendix A. Perturbed Probability Density

In this section, we evaluate a simple expression for the perturbed probability density of χ_k . We use Taylor series expansion up to the second order of infinitesimals

$$\frac{1}{\sqrt{1+x}} \cdot e^{-\frac{\alpha}{1+x}} = \frac{1}{e} \left(1 + \frac{(2\alpha-1)x}{2} + \frac{(4\alpha^2-12\alpha+3)x^2}{8} \right) \quad (\text{A.1})$$

Here we made the following variable change $a = -\frac{\chi_k^2}{2\lambda_k}$ and now equation (14) becomes

$$\begin{aligned} \rho_k(\chi_k|\hat{U}) &= \rho_k(\chi_k, \lambda_k + \lambda_{k,1} + \lambda_{k,2}) = \\ &= \frac{1}{\sqrt{2\pi(\lambda_k + \lambda_{k,1} + \lambda_{k,2})}} \exp \left[-\frac{\chi_k^2}{2(\lambda_k + \lambda_{k,1} + \lambda_{k,2})} \right] = \\ &= \frac{e^a}{\sqrt{2\pi\lambda_k}} \cdot \left(1 - \left(\frac{1}{2} + a \right) \frac{\lambda_{k,1}}{\lambda_k} - \left(a + \frac{1}{2} \right) \frac{\lambda_{k,2}}{\lambda_k} + \left(\frac{3}{8} + \frac{3}{2}a + \frac{a^2}{2} \right) \frac{\lambda_{k,1}^2}{\lambda_k} \right) = \\ &= \rho_k(\chi_k, \lambda_k) (1 + f_k(\chi_k, \hat{U})) \end{aligned} \quad (\text{A.2})$$

where the coefficients in the introduced correction $f_k = A(\hat{U}) + B(\hat{U})\chi_k^2 + C(\hat{U})\chi_k^4$ have the following form

$$\begin{aligned} A &= \frac{1}{\lambda_k} \left(-\frac{1}{2}\lambda_{k,1} - \frac{1}{2}\lambda_{k,2} + \frac{3}{8}\lambda_{k,1}^2 \right) \\ B &= \frac{1}{2\lambda_k^2} \left(\lambda_{k,1} + \lambda_{k,2} - \frac{3}{2}\lambda_{k,1}^2 \right) \\ C &= \frac{1}{8\lambda_k^3} \lambda_{k,1}^2 \end{aligned} \quad (\text{A.3})$$

Appendix B. Perturbed Entropy

In this section, we provide a detailed evaluation of the desired entropy. First, we will show that H_2 does not contribute to the entropy expression

$$H_2 = - \int d\chi \sum_{i \neq j} \langle f_i f_j \rangle_{\hat{U}} \prod_k \rho_k - \int d\chi \sum_i \ln(\rho_i) \sum_{i \neq j} \langle f_i f_j \rangle_{\hat{U}} \prod_k \rho_k \quad (\text{B.1})$$

Only the product of first-order corrections in A.3 leads to the expansion of $\langle f_i f_j \rangle$ up to the second order

$$\langle f_i f_j \rangle_{\hat{U}} = \frac{\langle \lambda_{i,1}, \lambda_{j,1} \rangle_{\hat{U}}}{\lambda_i, \lambda_j} \left(1 - \frac{\chi_i^2}{\lambda_i} \right) \left(1 - \frac{\chi_j^2}{\lambda_j} \right) \quad (\text{B.2})$$

The first term of H_2 decomposes to the sum of zero integrals product

$$\int d\chi \sum_{i \neq j} \frac{\langle \lambda_{i,1}, \lambda_{j,1} \rangle_{\hat{U}}}{\lambda_i, \lambda_j} \left(1 - \frac{\chi_i^2}{\lambda_i} \right) \left(1 - \frac{\chi_j^2}{\lambda_j} \right) \prod_k \rho_k = \quad (\text{B.3})$$

$$\begin{aligned} &= \sum_{i \neq j} \frac{\langle \lambda_{i,1}, \lambda_{j,1} \rangle_{\hat{U}}}{\lambda_i, \lambda_j} \int d\chi_i \rho_i \left(1 - \frac{\chi_i^2}{\lambda_i} \right) \int d\chi_j \rho_j \left(1 - \frac{\chi_j^2}{\lambda_j} \right) = \quad (\text{B.4}) \\ &= \sum_{i \neq j} \frac{\langle \lambda_{i,1}, \lambda_{j,1} \rangle_{\hat{U}}}{\lambda_i, \lambda_j} (1-1)(1-1) = 0 \end{aligned}$$

The second term is also the sum of vanishing products

$$\begin{aligned} &\int d\chi \sum_l \ln(\rho_l) \sum_{i \neq j} \langle f_i f_j \rangle_{\hat{U}} \prod_k \rho_k = \quad (\text{B.5}) \\ &= \sum_{i \neq j, l} \mathbb{E}_{\chi_l} \ln(\rho_l) \frac{\langle \lambda_{i,1}, \lambda_{j,1} \rangle_{\hat{U}}}{\lambda_i, \lambda_j} \int d\chi_i \rho_i \left(1 - \frac{\chi_i^2}{\lambda_i} \right) \int d\chi_j \rho_j \left(1 - \frac{\chi_j^2}{\lambda_j} \right) + \\ &+ \sum_{i \neq j} \frac{\langle \lambda_{i,1}, \lambda_{j,1} \rangle_{\hat{U}}}{\lambda_i, \lambda_j} \int d\chi_i \rho_i \ln(\rho_i) \left(1 - \frac{\chi_i^2}{\lambda_i} \right) \int d\chi_j \rho_j \left(1 - \frac{\chi_j^2}{\lambda_j} \right) = \\ &= \sum_{i \neq j} \mathbb{E}_{\chi_k} \ln(\rho_l) \frac{\langle \lambda_{i,1}, \lambda_{j,1} \rangle_{\hat{U}}}{\lambda_i, \lambda_j} (1-1)(1-1) + \\ &+ \sum_{i \neq j} \frac{\langle \lambda_{i,1}, \lambda_{j,1} \rangle_{\hat{U}}}{\lambda_i, \lambda_j} \int d\chi_i \rho_i \ln(\rho_i) \left(1 - \frac{\chi_i^2}{\lambda_i} \right) (1-1) = 0 \end{aligned}$$

Thus, the entropy expression (22) contains the following terms

$$\begin{aligned}
H &= - \int d\chi \left(1 + \sum_i \tilde{f}_i \right) \left(\sum_j \ln(\rho_j) + \sum_j \tilde{f}_j \right) \prod_k \rho_k = \quad (B.6) \\
&= - \int d\chi \sum_i \ln(\rho_i) \prod_k \rho_k - \int d\chi \sum_i \tilde{f}_i \prod_k \rho_k - \int d\chi \sum_i \ln(\rho_i) \sum_j \tilde{f}_j \prod_k \rho_k
\end{aligned}$$

One may integrate the second term in a way similar to 16 leading to

$$\int d\chi \sum_i \tilde{f}_i \prod_k \rho_k = \sum_i \int d\chi_i \rho_i \tilde{f}_i \quad (B.7)$$

We also write the third term as a sum of two terms. The first one is a product which contains incomplete sum for unperturbed entropy H_0 except the j -th term. The second term is also a product with the j -th term itself inside it

$$\begin{aligned}
& - \int d\chi \sum_i \ln(\rho_i) \sum_j \tilde{f}_j \prod_k \rho_k = \quad (B.8) \\
&= - \int d\chi \sum_{i \neq j} \ln(\rho_i) \sum_j \tilde{f}_j \prod_k \rho_k - \int d\chi \sum_j \ln(\rho_j) \tilde{f}_j \prod_k \rho_k = \\
&= \left(H_0 + \int d\chi_j \rho_j \ln(\rho_j) \right) \sum_j \int d\chi_j \rho_j \tilde{f}_j - \sum_j \int d\chi_j \rho_j \ln(\rho_j) \tilde{f}_j
\end{aligned}$$

Considering the above-mentioned simplifications we obtain the intermediate equation for the perturbed entropy

$$\begin{aligned}
H &= H_0 - \sum_i d\chi_i \rho_i \tilde{f}_i + \sum_i \int d\chi_i \rho_i \tilde{f}_i \left(H_0 + \int d\chi_i \rho_i \ln(\rho_i) \right) - \sum_i \int d\chi_i \rho_i \ln(\rho_i) \tilde{f}_i = \\
&= H_0 + \sum_i \mathbb{E}_{\chi_i} \left(\tilde{f}_i [H_0 - 1 + \mathbb{E}_{\chi_i} \ln(\rho_i)] \right) - \sum_i \mathbb{E}_{\chi_i} [\ln(\rho_i) \tilde{f}_i] \quad (B.9)
\end{aligned}$$

The final result is the function of only the averaged coefficients $\langle A \rangle_{\hat{U}}$, $\langle B \rangle_{\hat{U}}$ and $\langle C \rangle_{\hat{U}}$, which themselves are the functions of $\langle \lambda_{k,1} \rangle_{\hat{U}}$, $\langle \lambda_{k,2} \rangle_{\hat{U}}$, $\langle \lambda_{k,1}^2 \rangle_{\hat{U}}$

$$\begin{aligned}
H &= H_0 + \sum_i \left(H_0 - 1 + \int d\chi_i \rho_i \ln(\rho_i) \right) \int d\chi_i \rho_i \left(\langle A \rangle_{\hat{U}} + \langle B \rangle_{\hat{U}} \chi_i^2 + \langle C \rangle_{\hat{U}} \chi_i^4 \right) - \\
&\quad - \sum_i \int d\chi_i \ln(\rho_i) \left(\langle A \rangle_{\hat{U}} + \langle B \rangle_{\hat{U}} \chi_i^2 + \langle C \rangle_{\hat{U}} \chi_i^4 \right)
\end{aligned}$$

To find the expected value of terms in (B.9) one may use several common integrals [93]

$$\begin{aligned}
\mathbb{E}_{\chi_i} \ln(\rho_i) &= \int \frac{1}{\sqrt{2\pi\lambda_i}} e^{-\frac{\chi_i^2}{2\lambda_i}} \left(-\frac{\chi_i^2}{2\lambda_i} - \ln \sqrt{2\pi\lambda_i} \right) d\chi_i = \frac{1}{2} (-\ln(2\pi\lambda_i) - 1) \quad (\text{B.10}) \\
\mathbb{E}_{\chi_i} (\ln(\rho_i) \chi_i^2) &= -\frac{3}{2} \lambda_i - \frac{1}{2} \ln(2\pi\lambda_i) \lambda_i \\
\mathbb{E}_{\chi_i} (\ln(\rho_i) \chi_i^4) &= -\frac{15}{2} \lambda_i^2 - \frac{3}{2} \ln(2\pi\lambda_i) \lambda_i^2 \\
\mathbb{E}_{\chi_i} (\chi_i^2) &= \lambda_i \\
\mathbb{E}_{\chi_i} (\chi_i^4) &= 3\lambda_i^2
\end{aligned}$$

Substituting of common integrals into the expression for entropy we obtain

$$\begin{aligned}
H = H_0 + \sum_k \left[\left(-\frac{1}{2} \frac{\lambda_{k,1}}{\lambda_k} - \frac{1}{2} \frac{\lambda_{k,2}}{\lambda_k} + \frac{3}{8} \frac{\lambda_{k,1}^2}{\lambda_k^2} \right) \frac{1}{2} (-\ln(2\pi\lambda_k) - 1) + \right. \quad (\text{B.11}) \\
+ \left(\frac{1}{2} \frac{\lambda_{k,1}}{\lambda_k^2} + \frac{1}{2} \frac{\lambda_{k,2}}{\lambda_k^2} - \frac{3}{4} \frac{\lambda_{k,1}^2}{\lambda_k^3} \right) \left(-\frac{3}{2} \lambda_k - \frac{1}{2} \ln(2\pi\lambda_k) \lambda_k \right) + \\
\left. + \frac{1}{8} \frac{\lambda_{k,1}^2}{\lambda_k^4} \left(-\frac{15}{2} \lambda_k^2 - \frac{3}{2} \ln(2\pi\lambda_k) \lambda_k^2 \right) \right]
\end{aligned}$$

Simplifying the above equation we obtain the following final expression for entropy, which depends on the averaged eigenvalues corrections

$$H = H_0 + \frac{1}{2} \sum_k \left(\frac{\langle \lambda_{k,1} \rangle_{\hat{U}}}{\lambda_k} + \frac{\langle \lambda_{k,2} \rangle_{\hat{U}}}{\lambda_k} + 0 \cdot \frac{\langle \lambda_{k,1}^2 \rangle_{\hat{U}}}{\lambda_k} \right) \quad (\text{B.12})$$

Appendix C. Averaging Eigenvalue Corrections

In this section, we provide the exact expressions for the averaged eigenvalue corrections $\langle \lambda_{k,1} \rangle_{\hat{U}}$ and $\langle \lambda_{k,2} \rangle_{\hat{U}}$ over realizations of \hat{U} . While averaging of $\lambda_{k,1}$ and taking into account the zero expectation $\mathbb{E}(U(\mathbf{x})) = 0$ one may easily obtain

$$\langle \lambda_{k,1} \rangle_{\hat{U}} = \langle P_{kk} \rangle_{\hat{U}} = 0 \quad (\text{C.1})$$

where the matrix element of \hat{U} is defined in the following way

$$P_{km} = (\psi^k, \hat{U}\psi^m) = \sum_{ij} \psi_i^k \hat{U}_{ij} \psi_j^m \quad (\text{C.2})$$

Now let us consider the second-order correction to the eigenvalue

$$\lambda_{k,2} = \sum_{m \neq k} \frac{P_{km} P_{mk}}{\lambda_k - \lambda_m} \quad (\text{C.3})$$

According to our model of delta correlated values of random $U(x)$ in different points in space $\langle U(x)U(x+\tau) \rangle_{\hat{U}} = u(x)\delta(\tau)$ we suggest $\langle \hat{U}_{km} \hat{U}_{ln} \rangle$ is non-zero and equal to u_{ln} if and only if \hat{U}_{km} is the same as \hat{U}_{ln} or \hat{U}_{nl} which can be written as follows

$$\langle \hat{U}_{km} \hat{U}_{ln} \rangle = (\delta_{kl} \delta_{mn} + \delta_{kn} \delta_{ml}) u_{ln} \quad (\text{C.4})$$

Using this correlation model on entries of random matrix \hat{U} we can obtain the following expression for the product of matrix elements in $\lambda_{k,2}$

$$\begin{aligned} \langle P_{k,m} P_{m,k} \rangle &= \sum_{l,p} \left\langle \psi_l^k \sum_n \hat{U}_{l,n} \psi_n^m \psi_p^m \sum_s \hat{U}_{p,s} \psi_s^k \right\rangle_{\hat{U}} \\ &= \sum_{l,n,p,s} \psi_l^k \psi_p^m \psi_n^m \psi_s^k (\delta_{lp} \delta_{ns} u_{ln} + \delta_{ls} \delta_{np} u_{ln}) \\ &= \sum_{l,n} \psi_l^k \psi_l^m u_{ln} \psi_n^k \psi_n^m + \sum_{l,n} (\psi_l^k)^2 u_{ln} (\psi_n^m)^2 \end{aligned} \quad (\text{C.5})$$

Substitution of this result to the averaged second-order correction $\lambda_{k,2}$ leads to

$$\sum_k \frac{\langle \lambda_{k,2} \rangle}{\lambda_k} = \sum_k \frac{1}{\lambda_k} \sum_m \frac{\langle P_{km} P_{mk} \rangle}{\lambda_k - \lambda_m} \quad (\text{C.6})$$

$$= \sum_{k,m} \frac{1}{\lambda_k (\lambda_k - \lambda_m)} \sum_{l,n} (\psi_l^k \psi_l^m u_{ln} \psi_n^k \psi_n^m + (\psi_l^k)^2 u_{ln} (\psi_n^m)^2) \quad (\text{C.7})$$

Thus, the final expression for entropy becomes

$$H = H_0 + \sum_{k,m} \frac{1}{2\lambda_k (\lambda_k - \lambda_m)} \sum_{l,n} (\psi_l^k \psi_l^m u_{ln} \psi_n^k \psi_n^m + (\psi_l^k)^2 u_{ln} (\psi_n^m)^2) \quad (\text{C.8})$$

In the next section we'll provide some simplification of this expression.

Appendix D. Approximate Expression for the Entropy

Firstly it can be seen that \hat{U} is symmetric matrix with non negative entries: $U_{ij} \geq 0$ and $U_{ij} = u(|i - j|)$. This means \hat{U} can be presented in the following way

$$\hat{U} = \sum_r u_r \hat{D}_r \quad (\text{D.1})$$

$$\hat{D}_r = \begin{pmatrix} 0 & & 1 & & 0 \\ & \ddots & & \ddots & \\ 1 & & 0 & & 1 \\ & \ddots & & \ddots & \\ 0 & & 1 & & 0 \end{pmatrix} \quad (\text{D.2})$$

where we introduced matrix D_r with nonzero entries on r -diagonals. Thus, one may consider scalar products in the right hand side of C.7. We denote the first and the second terms in the r.h.s. by I_1 and I_2

$$I_1 = 2 \sum_r \sum_{i=0}^{N-r} \psi_{1+i}^k \psi_{1+i}^m u_r \psi_{r+i}^k \psi_{r+i}^m = 2 \sum_r u_r \sum_{i=0}^{N-r} x_i y_i \quad (\text{D.3})$$

$$\begin{aligned} I_2 &= \sum_r \sum_{i=0}^{N-r} \psi_{1+i}^m \psi_{1+i}^m u_r \psi_{r+i}^k \psi_{r+i}^k + \sum_r \sum_{i=0}^{N-r} \psi_{1+i}^k \psi_{1+i}^k u_r \psi_{r+i}^m \psi_{r+i}^m \\ &= \sum_r u_r \sum_{i=0}^{N-r} (x_i^2 + y_i^2) \end{aligned} \quad (\text{D.4})$$

Here we use the following notation $x_i = \psi_{1+i}^k \psi_{r+i}^m$ and $y_i = \psi_{1+i}^m \psi_{r+i}^k$. Next, with a help of the following simple inequality

$$2|x_i y_i| \leq |x_i^2 + y_i^2| = x_i^2 + y_i^2 \quad (\text{D.5})$$

it is easy to compare D.3 and D.4: $|I_1| < |I_2|$. Moreover, taking the constant values in matrix $U_{ij} = u$ results in $I_1 = 0$ and $I_2 = 1$ due to normality condition $(\psi^i \psi^j) = \delta_{ij}$.

These two arguments together with variety of numerical comparisons allow us to suggest that in most physically interesting cases I_1 can be neglected. Thus, we propose the following simplification for the exact expression for the entropy (C.8) considering only leading order term

$$H \approx H_0 + \sum_{k,m} \frac{1}{2\lambda_k(\lambda_k - \lambda_m)} \sum_{l,n} (\psi_l^k)^2 u_m (\psi_n^m)^2 \quad (\text{D.6})$$

Nevertheless direct expression C.8 still can be used in all desired cases instead of simplified version.